Reactor Opportunities for the Spheromak

E. B. Hooper, R. H. Bulmer, T. K. Fowler, D. N. Hill, H. S. McLean, C. A. Romero-Talamás, R. W. Moir, B. W. Stallard, R. D. Wood, S. Woodruff

April 18, 2003

U.S. Department of Energy

Lawrence
Livermore
National
Laboratory

DISCLAIMER

REACTOR OPPORTUNITIES FOR THE SPHEROMAK*

E. B. Hooper, R. H. Bulmer, [1]T. K. Fowler, D. N. Hill, H. S. McLean,
[2]C. A. Romero-Talamás, R. W. Moir, B. W. Stallard, R. D. Wood, and S. Woodruff

Lawrence Livermore National Laboratory
Livermore, CA 94551 USA

[1]University of California
Berkeley, CA 94720, USA

[2]California Institute of Technology
Pasadena, CA 91125 USA

ABSTRACT

Experimental results from the Sustained Spheromak Physics Experiment, SSPX, are reviewed and applied to published reactor configurations. The results include several important features, including low fluctuation levels, (apparent) good magnetic flux surfaces, and moderate beta. Additional features needed for an attractive reactor but not yet demonstrated experimentally are identified by comparison with the reactor designs, and possible alternatives to a fully steady-state device are discussed.

INTRODUCTION

The spheromak [1, 2] is a self-organized, toroidal plasma with unique features offering promising reactor opportunities. The plasma is confined with both toroidal and poloidal magnetic fields; there are no toroidal field windings or a transformer, and thus no central stack threading the plasma torus so the vacuum chamber is singly connected. A poloidal bias magnetic field is applied and, in steady-state versions of a reactor, a vertical magnetic field to handle the hoop stress. (In pulsed versions, this field is generated by induced currents in the flux conserver surrounding the plasma.) However, this geometric simplicity leads to complex physics. As with the RFP the safety factor in the plasma is usually less than one. The current is driven by injection of magnetic helicity; this breaks the magnetic flux surfaces so thermal energy leaks across the magnetic field during current drive. The critical issue then is to confine a thermonuclear plasma sufficiently well for energy generation while building and sustaining the magnetic field [3]. The resultant reactor, either pulsed or steady state, would then be potentially an excellent candidate for power generation.

The Sustained Spheromak Physics Experiment, SSPX (Fig. 1), was proposed [4] and constructed as a "Concept Exploration experiment" to study the physics of the spheromak and to determine whether there are paths forward which hold sufficient promise for fusion energy to warrant a "Proof of Principle experiment" on the concept. Results and supporting
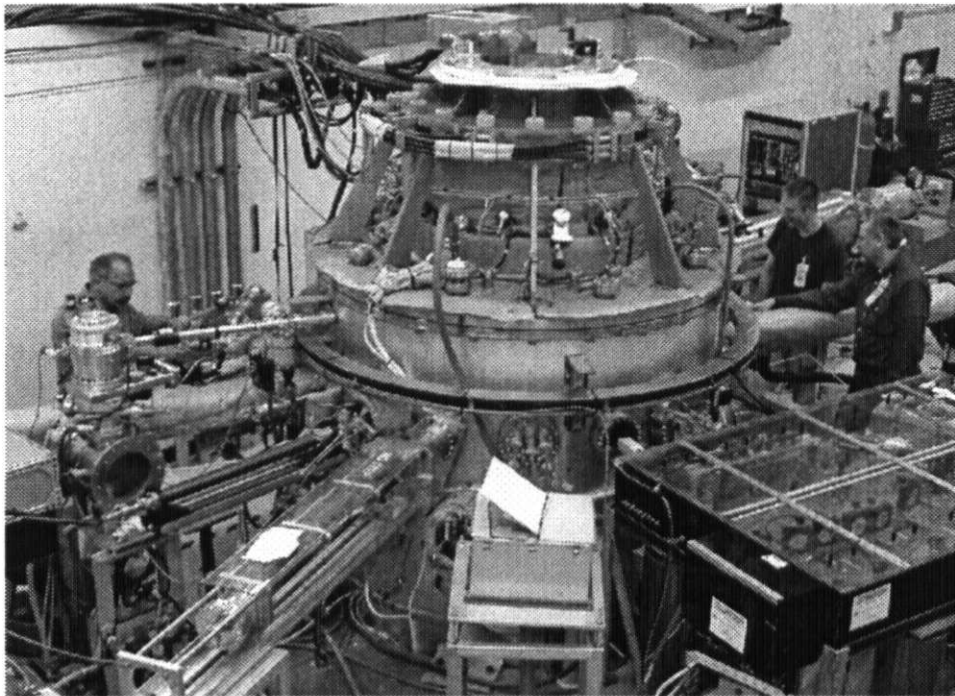
1

Fig. 1. The SSPX experiment uses a wide range of diagnostics to determine the magnetic field and its structure, the electron density and temperature, magnetic fluctuations, and other experimental data in a spheromak generated by coaxial helicity injection.

understanding to date are promising. Results are summarized in this report, including the constraints on $\lambda = \mu_0 j/B$, with B the magnetic field and j the current density along B, and its roles in obtaining high quality plasmas [5]. As with the RFP, the gradient in this parameter determines the stability of tearing modes and thus the quality of the magnetic flux surfaces; in addition, in the spheromak flattening the gradient can ensure that the safety factor is not the ratio of low integers, thus improving stability to ideal MHD modes. Experiments demonstrate that if this parameter has weak gradients, "good" flux surfaces, defined as supporting peaked electron temperature profiles, are present in the plasma. Initial results included central electron temperatures up to 120 eV [6]; since then, temperatures of 200 eV have been sustained for > 1 ms [7]. These and other results provide the basis for extrapolation to possible reactors.

Reactor studies which provide visions for the energy goal can be evaluated in light of the new results. Hagenson and Krakowski [8] (hereafter "H&K") described a toroidal reactor with an outside plasma radius 1.7 to 3 m and no central column. A neutron wall power density close to 20 MW/m^2 was assumed, and the thermonuclear core of the reactor replaced regularly, taking advantage of the singly-connected geometry. In the present understanding of neutron damage, this high flux will likely have to be reduced and mitigation of materials damage will be required. Never-the-less, this is a good starting point for a "standard" reactor with significant differences from a tokamak. Other reactor visions depart significantly from a "tokamak-like" power plant. Perkins considered a "boiling pot" reactor [9] in which the first wall is surrounded by liquid lithium (to generate tritium) with an admixture of sodium and potassium, which evaporated and carried the heat to a turbine. Recognizing the gains to follow from protecting solid walls from neutrons, Fowler, et al. [10], considered a pulsed reactor with lithium walls which were expelled by plasma pressure following a rapid plasma burn. Hooper and Fowler proposed a steady state reactor with liquid walls; later, Moir et al. [11] generated a design of a steady state reactor with the walls protected by flowing liquid salt or metal [12]. Although further effort is needed to make this design fully self consistent, it demonstrated the promise of such a device. Bourque, et al., [13] considered a reactor driven by repetitive merging of spheromaks.

Absent a fuller understanding of spheromak physics, these designs must be considered illustrative of what might be achievable rather than true designs; nevertheless, they provide a basis for exploring possible paths to eventual reactors. These paths, and the resulting implications for required physics experiments, are discussed here with particular attention to the designs of H&K, Moir et al., and Fowler, et al.

EXPERIMENTAL RESULTS

A cross section of the SSPX experiment is shown in Fig. 2a, which shows an example of the axisymmetric MHD approximation to the equilibrium in the flux conserver. Figure 2b is a photograph of the discharge early in time (when atomic-light emission is high), clearly showing the discharge current path along the geometric axis of the spheromak. Two features of the "flux-core" spheromak are immediately apparent: The importance of the current on the open fieldlines and the major role of the flux conserver in determining the magnetic equilibrium. The currents on the open fieldlines determine the boundary condition for fields at the spheromak separatrix and transport magnetic helicity from the injector to drive current in the spheromak. At the electrically conducting flux conserver, the normal component of the magnetic field is zero. Currents flowing in the wall provide the vertical field necessary to support the spheromak loop stress and provide stability against the tilt and shift modes of the spheromak. The experimental pulse length is short enough that decay of these currents is not a major issue for the equilibrium.
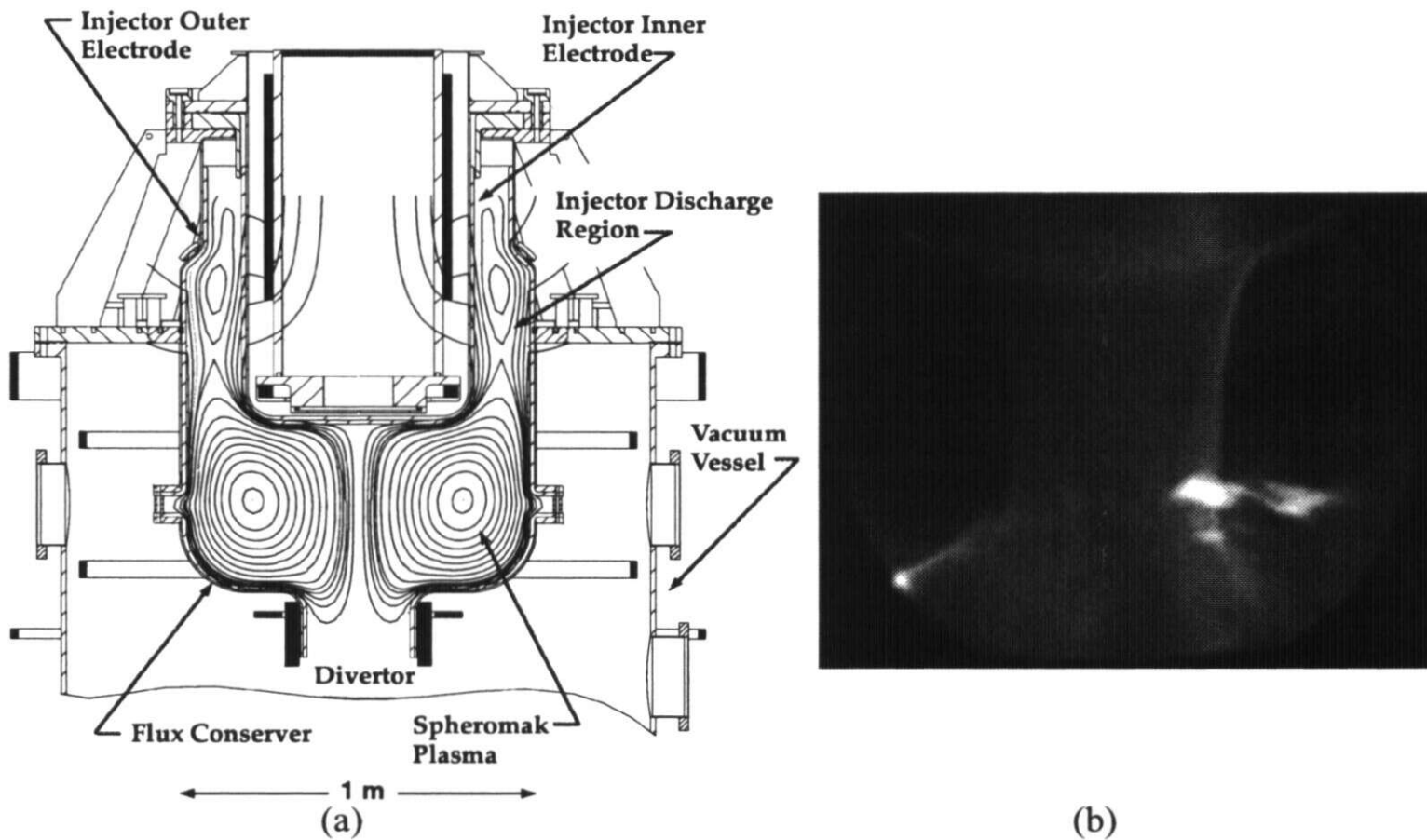
Fig. 2. (a) Spheromak equilibrium and vessel cross section. (b) Photograph of the discharge showing the central flux core.

The experimental key to obtaining high electron temperatures in SSPX has been to adjust the values of the bias (gun) magnetic flux, Φ_{gun}, and the gun current, I_{gun}, so that their ratio, $\lambda_{gun} = \mu_0 I_{gun}/\Phi_{gun}$ is close to the lowest eigenvalue for the spheromak flux conserver. (The eigenvalue is defined as the homogeneous solution to $\nabla \times \mathbf{B} = \lambda_{fc}\mathbf{B}$ in the flux conserver, with λ_{fc} = constant.) It can be shown that in the dissipationless limit the flux amplification approaches infinity for operation when λ within the flux conserver is constant and approaches λ_{fc} [2, 5, 14] Such operation thus naturally satisfies the Taylor condition for minimizing the spheromak energy at a constant magnetic helicity [15], it is also the condition for eliminating the free-energy associated with current-driven tearing modes in the spheromak [16].

Fig. 3. Time history of two high temperature discharges. Shot 9779 used H_2 as the operating gas; 10074 used He. Shown (top-to-bottom) are (a) Gun Current (A). Note that discharge 10074 started earlier in dischar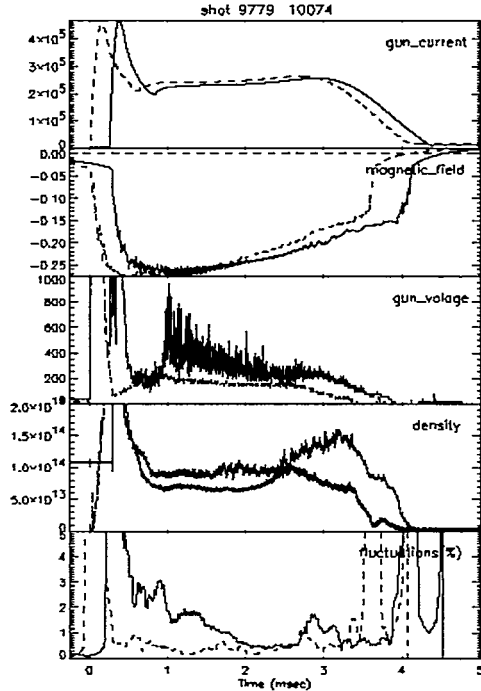ge time than 9779. (b) The magnetic field (T) at the flux conserver midplane. (c) Gun voltage (V). (d) Line-averaged density (cm^{-3}). (e) Magnetic field fluctuation level (%) at the flux conserver midplane.
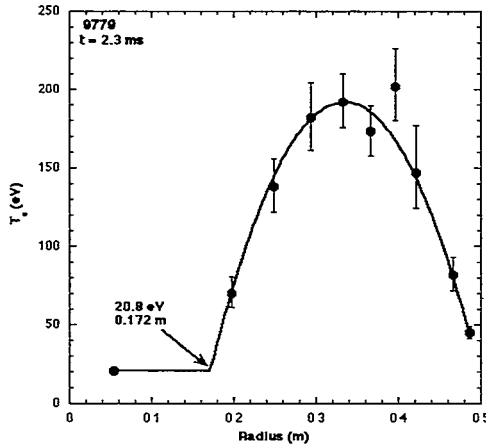
Fig. 4. Electron temperature profile [17] for a high T_e shot. The edge temperature in SSPX discharges is observed to range from 20 eV to 40 eV.

An example of SSPX operation at near-constant λ is shown in Fig. 3 [17]. The magnetic fluctuation level at the wall is in the range of 0.5-2% during much of the discharge. Thomson scattering measurements show that the density for this discharge, 6-8×10^{20} m^{-3} has an approximately flat profile; the electron temperature at a time of low fluctuation level, Fig. 4, is strongly peaked inside the separatrix (described below) suggesting that the magnetic flux surfaces are effectively closed.

Magnetic field modeling of discharges in SSPX includes fitting of the magnetic probes, Fig. 5a, at the flux conserver wall with a 2-dimensional MHD equilibrium. [5] The result, Fig. 5b, yields the location of the magnetic separatrix (neglecting the effects of 3-dimensional structures) at 0.125 m, approximately half way between the data point near the geometric axis and the break in the curve chosen for the fit. Also shown on the figure is the break-point from the temperature fit; it is clear that the last closed flux surface lies at a major radius equal to or less than this point. The measurements and the fit are thus

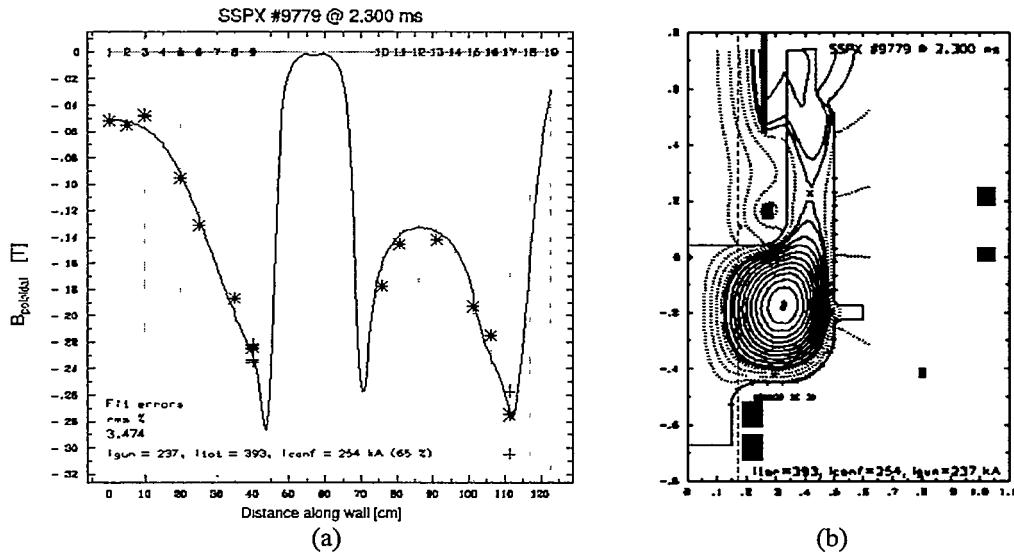Fig. 5. (a) Axisymmetric MHD fit to the magnetic field profile on the wall. (Shot 9779 at 2.3 ms.) (b) Fig. 6. Equilibrium corresponding to Fig. 5. The temperature-fit break point (dashed line) is likely the maximum radial location of the last closed flux surface.

consistent; in the future, electron temperature measurements will be made closer to the separatrix radius predicted by the fitting. The magnetic field at the wall midplane is measured to be 0.21 T at the time of the Thomson scattering measurement, corresponding to a field at the magnetic axis of 0.4 T, as determined by the fits. (Other discharges are estimated to reach up to 0.6 T at the magnetic axis.) The resulting peak electron beta is > 4%; assuming that the ions have the same temperature, a peak total beta of > 8% is obtained for this discharge.

The profiles of λ and resulting safety factor, q, resulting from the magnetic fit to a discharge at the Thomson scattering time (2.3 ms) are shown in Fig. 7a. Consistent with the above picture, λ is almost flat. Furthermore, q does not cross a low-order rational surface except near the separatrix, so there are no low mode-number rational surfaces in the core of the discharge. In contrast, a plot from early in time during a similar discharge is shown in Fig. 7b. The λ-profile dips deeper, consistent with the picture of fluctuations resulting from resistive mode drive, and the q-profile crosses 3/4 in the core.
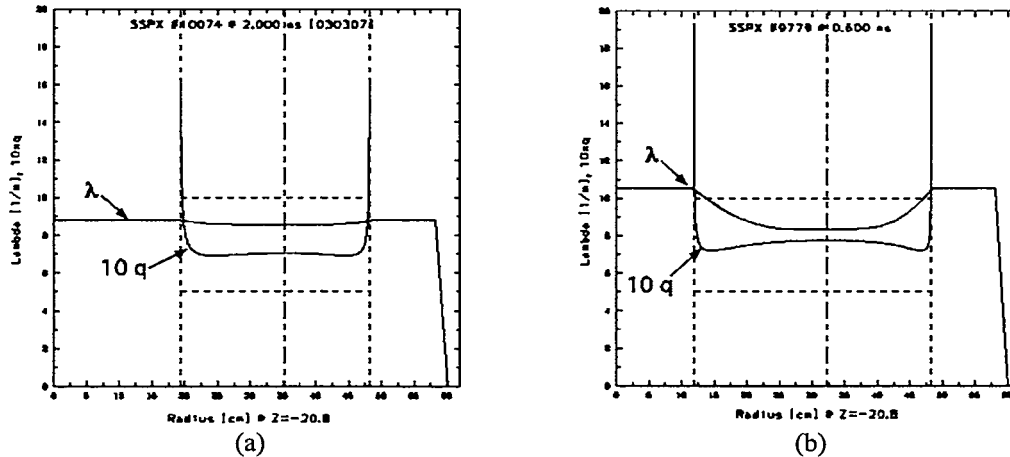

Fig. 7. (a) Profiles of λ and q in a high-temperature discharge. (b) Profiles early in a discharge when fluctuation levels are high and temperature is low. Compare with Fig. 3.
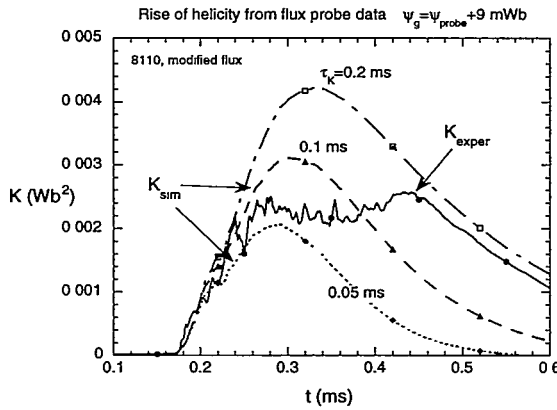
5

Fig. 8. Helicity content in a SSPX discharge, compared against a simple helicity balance model at several helicity loss rates [18].

The magnetic field in these discharges is generated during the formation stage of the discharge when fluctuations are high and fieldlines are apparently open throughout the entire volume, and electron temperatures are low, typically 40 eV. The magnetic energy then decays at a rate roughly twice the classical L/R time of the toroidal plasma. Thelater decay is consistent with the expectation that helicity transport into the core plasma, needed to sustain the current through the dynamo effect, is low or nonexistent at these low fluctuation levels. We conclude that at values of λ_{gun} significantly higher than λ_{fc}, helicity transport describes successful current drive, but the surfaces apparently open so extensively that thermal losses reduce the electron temperature to well under 100 eV. An example is shown in Fig. 8, where the measured helicity content is compared with a simple buildup model [18]. During the initial buildup the injection of helicity is much larger than the losses. However, once the magnetic fluctuations become substantial, the loss time becomes 0.05-0.1 ms, consistent with ohmic helicity losses calculated at the predicted rate of twice the resistive loss rate. Later in the discharge, the plasma becomes quieter and the loss time increases as the current dies away. Similar conclusions result from current drive described using a hyper-resistivity model [19].

The electron thermal diffusivity estimated, at 30 m²/s at 120 eV by balancing ohmic heating against thermal losses [20], reduces to ~ 10 m²/s at 200 eV. This is considerably less than Bohm diffusion, $6.25\times10^{-2}T_e/B \approx 30$ m²/s at 200 eV and 0.4 T. Rechester-Rosenbluth diffusion [21], with an electron thermal conductivity given by

$\chi_{e,RR} = L_c v_e \left| \tilde{B}/B \right|^2$ ($\tilde{B}$ is the fluctuation level), arises when magnetic fields are stochastic

and flux surfaces poorly defined. At the plasma edge in the discharge shown, $\left| \tilde{B}/B \right| \approx 1\%$; the actual value in the plasma interior is uncertain. Setting $\chi_{e,RR} = 10$ m²/s at 200 eV yields a parallel correlation length, L_c, of 1.4×10^{-2} m, much less than the flux conserver radius of 0.5 m. This short length is inconsistent with the assumptions of the model; either any fieldline stochasticity is isolated, the magnetic fluctuation level in the plasma core is much less than on the wall, or the measured fluctuations on the edge are not related to fieldline tearing and the model does not apply with their fields. If the field is stochastic in the core with $L_c \approx \pi R = 1.5$ m, then a core fluctuation level of $\left| \tilde{B}/B \right| \approx 10^{-3}$ is implied.

IMPLICATIONS OF EXPERIMENTAL RESULTS

A detailed reactor study of a steady-state spheromak (Fig. 9) sustained by helicity injection (from a coaxial plasma gun) was undertaken by H&K [8] in the mid-1980s, who stated "A range of cost-optimized reactor design points is presented, and the sensitivity of cost to key physics, engineering, and operational variables is presented." The conclusion
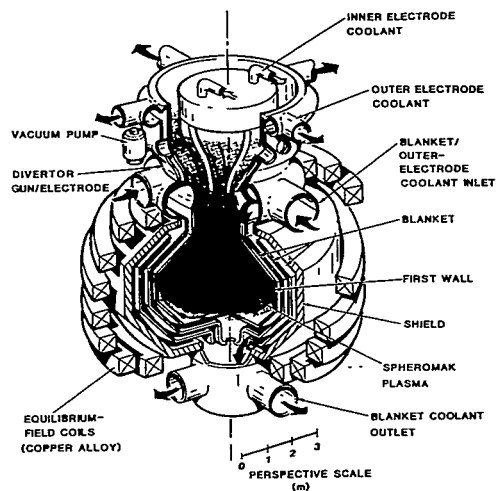
Fig. 9. Reactor design by H&K [4]. This is a steady-state device operating at 1 GWe (net).

was that the potential existed for a compact reactor with cost of electricity (COE) in the range of 40-100 mills/kWatt(electric)-hour and an electrical output ~ 1 GWe. At the lower end, at least, these costs are competitive, offering considerable incentive for research. The lack of toroidal coils linking the vessel allows for relatively easy removal of the plasma facing components. The dose limit of the first wall was taken to be 15 MW-yr/m^2 and the change-out time of the fusion power core estimated at 28 days; the minimum cost design then was found to have a neutron flux close to 20 MW/m^2. This was made possible by factory production of the thermonuclear core.

H&K also identified areas of significant physics uncertainty as transport and the need for high electron temperatures in the edge plasma to reduce ohmic losses. Further, they found that the flux within the spheromak separatrix needed to be ~ 100 times the bias flux applied by the gun in order that the ohmic losses in the edge plasma be low enough to allow high efficiency power production. Experimental progress towards these and other requirements is summarized as follows:

1) *Operation at constant λ is needed for efficient operation.* This has been demonstrated in SSPX and leads to low magnetic fluctuations as expected.

2) *Mechanisms of helicity generation, transport, and absorption need to be understood.* Progress has been made experimentally and is in agreement with the use of helicity as a paradigm for describing current drive in the spheromak, although more work is needed to determine details and the range of conditions for which the description is accurate. Progress has been made on models, both with the helicity mechanism and based on more fundamental physics (resistive MHD).

3) *Low energy transport across the mean-field magnetic flux surfaces is necessary for reactor operation.* Results from SSPX are optimistic, with the core electron thermal conductivity approaching the level of L-mode scaling in the tokamak. Achieving T_e = 200 eV in SSPX with a minor radius of only 15-20 cm. is strongly suggestive that fusion level temperatures are feasible in a larger, higher magnetic field device. However scaling to fusion temperatures is not demonstrated, and the detailed physics of the transport is not experimentally confirmed. Further, and perhaps most importantly, sustainment and building of the magnetic field has not been demonstrated simultaneously with low energy losses. This is an important feature of a steady-state reactor [3].

4) *Plasma beta ~ 10% is required.* There has been significant experimental progress towards achieving this goal. Plasma peak betas of 8% (assuming $T_i = T_e$) have been

7

achieved in low fluctuation level spheromaks. Transient peak electron betas of 20% have been observed [22].

5) *Open magnetic flux must be < 0.01 of the closed flux.* This issue is closely related to the flux amplification. Achieving high flux (and current) amplification has not yet been demonstrated. On SSPX, current amplifications (I_T/I_{gun}) of 2.5 have been achieved, and CTX reached a factor of 3 [1]. The physics determining this factor are a central part of ongoing research. It is clear that the amplification factor is sensitive to the geometry of the vacuum bias magnetic flux and the details of the helicity drive, suggesting than more than one mechanism may be operating in the experiment [23], suggesting a path towards higher amplification. If it is concluded that the amplification factor is low for fundamental reasons, a pulsed reactor may be a better approach to power production than a steady-state device, as the drive power need only be high during the initiation of the plasma and may be significantly reduced during the burn phase. Alternatively, repetitive pulsing followed by a "coasting" burn period might offer net energy gain; such operation is sometimes termed "refluxing" [24].

6) *High electron edge temperatures are required to minimize ohmic heating losses.* The edge electron temperature is found to be 0.25-0.4 times the discharge voltage, in agreement with modeling on open magnetic fieldlines. Fusion (alpha-particle) power will enhance this significantly; it thus appears likely that the necessary edge temperatures can be reached.

7) *A method of handling power in the divertor is needed which is consistent with high edge temperature.* Although this has not been addressed experimentally, the liquid-wall reactor design by Moir, et al., discussed below, describes a plausible solution.

Neutron damage to reactor walls and components could be significantly alleviated by a thick, neutron absorbing layer of liquid salt or tin-lithium metal facing the plasma. Because the magnetic field from the plasma is purely poloidal at the wall, the flow of this liquid is almost along fieldlines, so that MHD impedance is not a significant issue. Moir et al. [11] conducted a relatively detailed design, resulting in the reactor shown in Fig. 10. To ensure high beta as evaluated by the Mercier limit, they assume the λ-profile shown in Fig. 11; it remains to be seen whether magnetic or velocity shear can will be sufficiently high in this configuration to eliminate plasma instabilities.
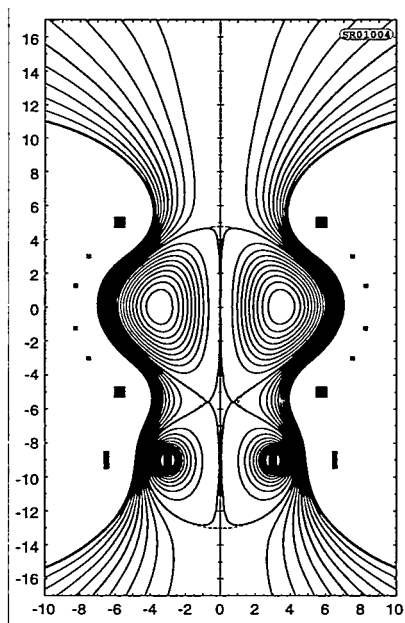

Fig. 10. Reactor with a thick flowing liquid wall; design by Moir, et al. [11]
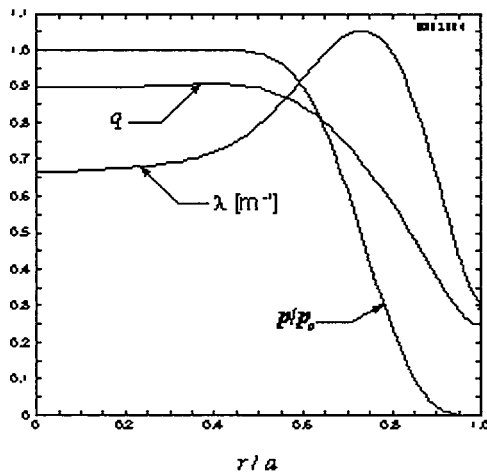
Fig. 11. Profiles in the liquid-wall reactor, yielding volume-averaged beta > 10%.
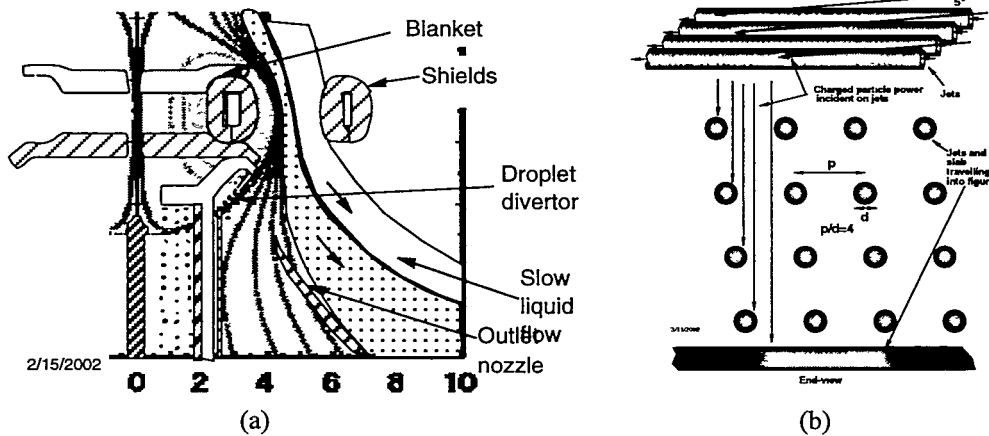

(a)   (b)

Fig. 12. (a) Configuration of the liquid wall reactor in the divertor section. (b) Liquid-drop spray to handle the power and protect solid surfaces.

Moir, et al. propose a potential solution to the divertor heat problem posed by H&K. A liquid-drop spray, shown in Fig. 12, would absorb the exhaust power while protecting the surface from damage. The feasibility of this solution is currently under investigation as part of the technology activities in the US Fusion Energy Program. In general, technology issues associated with liquid walls are in an early stage of development and will need attention.

Most of the comments applying experimental results to the H&K reactor design also apply here. The possible use of molten salt raises an additional one:

8) *Control of tilt and shift modes may be difficult for liquid salt walls.* For solid and liquid conducting (metal) walls the spheromak tilt and shift modes become resistive wall modes with slow growth rates which can be handled by feedback techniques similar to those being developed to maximize the beta of advanced tokamaks. However, for salt the conductivity is low and the corresponding growth rate is large and may be difficult to control. (In the experiment, timescales are short enough that they are fully controlled by the conducting wall.)

As discussed above, a pulsed reactor may be more attractive than a steady-state device. A concept using liquid-lithium walls (Fig. 13) was explored by Fowler, et al. [10].
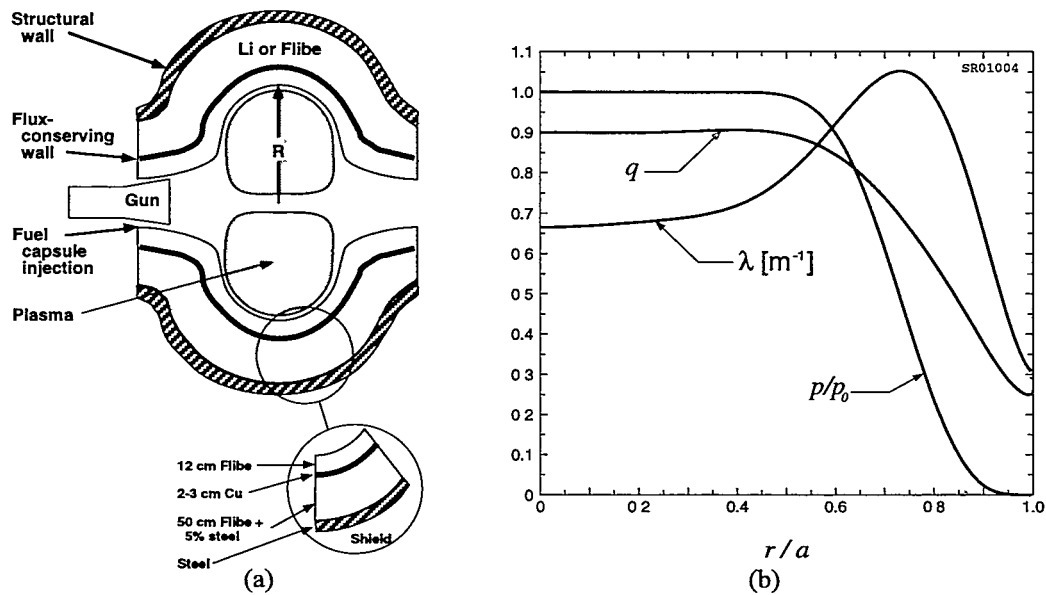
9

Fig. 13. (a) Pulsed reactor design [10]. (b) Profiles in a high-beta, pulsed reactor.

In this concept, the magnetic field is built up by high gun currents at relatively low T_e. When the drive is reduced, the magnetic flux surfaces heal and the plasma heats to fusion temperatures. This mode of operation is similar to the high-temperature operation achieved in experiments, although the device size and level of power injected are obviously of a different scale. When sufficiently high temperatures are reached, D-T fuel is injected and the burn part of the pulse initiated. This requires that particle confinement be comparable to energy confinement; its value is not well determined by present experiments. Tilt and shift modes grow (resistively) too slowly to reach significant amplitude, as in present experimental operation.

Both low beta (10-20%) and high beta (> 60%) scenarios were worked out. For the latter, the plasma current profiles are a strong example of the effect used by Moir, et al., as shown in Fig. 14. The λ-profile is nearly flat over more than 90% of the magnetic flux, yielding stability to low order core modes, and a boundary layer develops with a rapid variation which leads to strong magnetic shear and thus stability within the Mercier approximation. (The example yields 65% beta.) The plasma burn of the injected fuel is anticipated to proceed rapidly enough that residual tearing modes do not develop to high amplitude. These stability requirements have not yet been fully established in existing experiments.

The plasma burn increases the pressure rapidly, expelling the liquid wall to an heat exchanger. The cycle restarts by injection of liquid into the device, followed by the power cycle described above. The heat capacity of the liquid smoothes out time variations in the heat-conversion equipment, minimizing damage due to thermal cycling.

SUMMARY

Much of the physics required for a spheromak reactor has been successfully validated within the parameter levels achievable in a relatively small experiment such as SSPX. This includes operation at low fluctuation levels, apparently good flux surfaces, reduction of core electron thermal transport to levels comparable to those achieved in tokamaks of a similar size, moderate beta, and an understanding of electron temperature scaling on the open fieldlines in the edge plasma. The major qualitative uncertainties are the flux and current amplification, essential feature for a power reactor, and sustainment of high

temperatures during the buildup phase. Further understanding of all these issues at a level leading to predictive scaling is being pursued with the goal of evaluating possible future experimental facilities and quantifying reactor options. Pulsed reactor concepts suggest a path forward if either of major uncertainties are and do not satisfy the requirements for steady-state concepts.

References

*Work performed under the auspices of the U. S. Department of Energy by University of California Lawrence Livermore National Laboratory under contract No. W-7405-Eng-48.
1. T. R. Jerboe, Plasma Phys. Control. Fusion **36**, 945 (1994).
2. Paul M. Bellan, *Spheromaks* (Imperial College Press, London 2000).
3. T. K. Fowler, Fusion Techn. **29**, 206 (1996).
4. E. B. Hooper, J. H. Hammer, C. W. Barnes, J. C. Fernández, and F. J. Wysocki, Fusion Techn. **29**, 191 (1996).
5. E. B. Hooper, L. D. Pearlstein, and R. H. Bulmer, Nucl. Fusion **39**, 863 (1999).
6. H. S. McLean, S. Woodruff, E. B. Hooper, R. H. Bulmer, D. N. Hill, C. Holcomb, J. Moller, B. W. Stallard, R. D. Wood, Z. Wang., Phys. Rev. Letters **88**, 125004 (2002).
7. SSPX Experimental Team, private communication (2003).
8. R. L. Hagenson and R. A. Krakowski, Fusion Techn. **8**, 1606 (1985); LANL Report LA-10908-MS, March 1989.
9. L. J. Perkins, private communication (1996).
10. T. K. Fowler, D. D. Hua, E. B. Hooper, R. W. Moir, and L. D. Pearlstein, Comments Plasma Phys. and Controlled Fusion, **1** Part C, 83 (1999).
11. R. W. Moir, R. H. Bulmer, T. K. Fowler, T. D. Rognlien, and M. Z. Youssef, to be published.
12. E. B. Hooper and T. K. Fowler, Fusion Techn. **30**, 1390 (1996); T. K. Fowler and E. B. Hooper, Proc. 8th Intern. Conf. Emerging Nuclear Energy Systems, Obninsk, Russia, June 24-28 (1996).
13. R. F. Bourque, P. B. Parks, and M. J. Schaffer, ICC Workshop, College Park, MD, 22-24 Jan. 2002; see https://wormhole.ucllnl.org/ICC2002/.
14. T. H. Jensen and M. S. Chu, Phys. Fluids **27**, 2881 (1984).
15. J. B. Taylor, Phys. Rev. Letters **33**, 1139 (1986); Rev. Mod. Phys. **58**, 741 (1986).
16. A. H. Boozer, in *Encyclopedia of Physical Science and Technology*, (Academic Press, N. Y. 1992), Vol. 13, p. 1.
17. H.S. McLean, D.N. Hill, R.H. Bulmer, B.I Cohen, E.B. Hooper, J. Moller, D.D. Ryutov, B.W. Stallard, R.D. Wood, and S. Woodruff, 30th EPS Conference on Plasma Phys. and Contr. Fusion, St. Petersburg, Russia, July 7-11, 2003.
18. B. W. Stallard, S. Woodruff, R. H. Bulmer, D. N. Hill, E. B. Hooper, H. S. McLean, R. D. Wood, Physics of Plasmas, to be published.
19. E. B. Hooper and L. D. Pearlstein, Plasma Phys. Reports **28**, 705 (2002).
20. D. N. Hill, R. H. Bulmer, B. I. Cohen, E. B., Hooper, H. S. McLean, J. Moller, L. D. Pearlstein, D. D. Ryutov, B. W. Stallard, R. D. Wood, S. Woodruff, IAEA Conf., Lyon, France Oct. 2002, paper EX/C1-3.
21. A. B. Rechester and M. N. Rosenbluth, Phys. Rev. Letters **40**, 38 (1978).
22. F. J. Wysocki, J. C. Fernández, I. Henins, T. R. Jarboe, and G. J. Marklin, Phys. Rev. Letters **61**, 2457 (1988).
23. S. Woodruff, D.N. Hill, B.W. Stallard, R. Bulmer, B. Cohen, C.T. Holcomb, E.B. Hooper, H.S. McLean, J. Moller, R.D. Wood, Phys. Rev. Letters **90**, 095001-1 (2003).
24. T. R. Jarboe and S. Woodruff, private communication.